Theoretical Treatment for Electron Transport throughout Benzene Ring Model
معالجة نظرية لنقل الإلكترون خلال نموذج حلقة البنزين

م.م.لافي فرج البدري وأ.د. جنان مجيد المخ وأ.د.شاكر أبراهيم عيسى
قسم الفيزياء\كلية التربية للعلوم الصرفة\جامعة البصرة

Abstract

In this paper we present our theoretical treatment for electron transport through benzene ring attached to donor and left lead in the left side, while in the right side it is attached to acceptor and right lead. Our treatment is based on the time-dependent Anderson – Newns Hamiltonian. The equations of motion are derived for all subsystems then the steady state is considered to obtain analytical expression for the transmission probability as a function of system energies. The subsystems eigenvalues, the coupling interaction between them as well as the leads band width all are taken into consideration and highlighted. We concluded that the variation of contact's position of the acceptor with the benzene ring may have great effects on the electronic transport properties of molecular devices because of quantum interference.

الملخص

نقدم في هذا البحث معالجتنا النظرية لنقل الإلكترون خلال حلقة بنزين مربوطة إلى واهب وقطب أيسر في الجانب الأيسر، بينما في الجانب الأيمن فهي مربوطة إلى قابل وقطب أيمن. معالجتنا أسست على هاملتونين أندرسون –نيونس المعتمد على الزمن. تم أشتقاق معادلات الحركة لكل أجزاء النظام ثم أعتبرت الحالة المستقرة من أجل الحصول على تعبير تحليلي لأحتمالية النفاذية كدالة لطاقات النظام. تم الأخذ بنظر الأعتبار القيم الذاتية لأجزاء النظام وتفاعل الأزدواج بينها فضلاً عن عرض حزمة الأقطاب . نستنتج أن تغيير موقع ربط القابل مع حلقة البنزين قد يكون له تأثيرات عظيمة على خواص نقل الألكترون للأجهزة الجزيئية بسبب التداخل الكمي.

1- Introduction

Among recent developments, devices using single molecules as nanoscale conductors have attracted great attention. Many theoretical and experimental studies have been reported concerning the molecular devices, because of expected exotic properties particular to small molecules, which are considered to be an ultimate goal in the miniaturization of electronic devices [1,2]. Therefore, an understanding of the electron transport properties through a single molecule is indispensable to develop a single molecular device [2]. The contact details at the electrode–molecule interface may have great effects on the electronic transport properties of molecular devices [3,4]. Among features of the electron transport properties is quantum interference of electronic waves associated with the geometry of the bridging system [1].

Interference effects have been the subject of extensive research [5]. The appearance of quantum interference in the microscopic world is one of the deepest mysteries at the very root of quantum mechanics [6]. Interference is one of the fundamental properties of quantum systems. Mesoscopic systems have provided a useful ground to study quantum interference phenomena since the pioneering experiments [7]. A distinctive feature of electron tunneling through quantum dots is the retention of the quantum phase coherence. For this reason, multiple connected geometries involving quantum dots exhibit quantum interference phenomena, such as the Fano effect [1], which arises from the interference between a discrete state and a continuum [8]. The reduction of size in the electronic devices to nanometer scale has highlighted the importance of the effects of quantum coherence and interference. The control of such effects is important to provide both a better

understanding of the quantum realm as well as new functionalities to the circuits. Quantum interference allows to enhance or to cancel, total or partially, the response of the system beyond the simple classical additive behavior. Such an effect can pose a problem to be avoided but also could provide new capabilities to the device with respect to its classical counterpart [9].

Among mesoscopic conductors, ring shaped devices [10] (often called *quantum rings*) are intensely studied due to their ability to show various types of quantum interference phenomena, such as the well-known Aharonov-Bohm effect [11,12,13], when the wave function of a charged particle passing around a magnetic flux experiences a phase shift as a result of the enclosed magnetic field. The interference is produced by electrons which travel coherently along the two arms of the ring. Part of the electrons may suffer inelastic collisions along their motions.

The Aharonov-Bohm effect occurs when charge carriers are passed through a ring, where two separate paths of almost equal length are possible for these carriers. As they meet at the other side of the ring, if the distance traversed is less than the coherence length, interference effects appear as a function of magnetic field [5].

In this work, we will present our theoretical treatment to formulate expression for the electron transport throughout benzene ring model to study and calculate the electronic properties for the considered system. So, all the system eigenvalues and coupling interactions are taken into consideration to give obvious view for the system dynamics. In this paper, we investigate the quantum interference effect mechanism by performing quantum transport calculations for benzene ring model threaded by an Aharonov-Bohm (AB) flux.

2- Theory

In this work, the considered system is left lead-donor-benzene ring-acceptor-right lead, where the benzene ring model consists of six quantum dots. General formula for the transmission probability for the benzene ring model, threaded by a magnetic flux, will be derived for the system shown in Fig.(1), this system is described by using time-dependent and spin less Anderson – Newns Hamiltonian [15], which neglects Coulomb interactions in all subsystems.

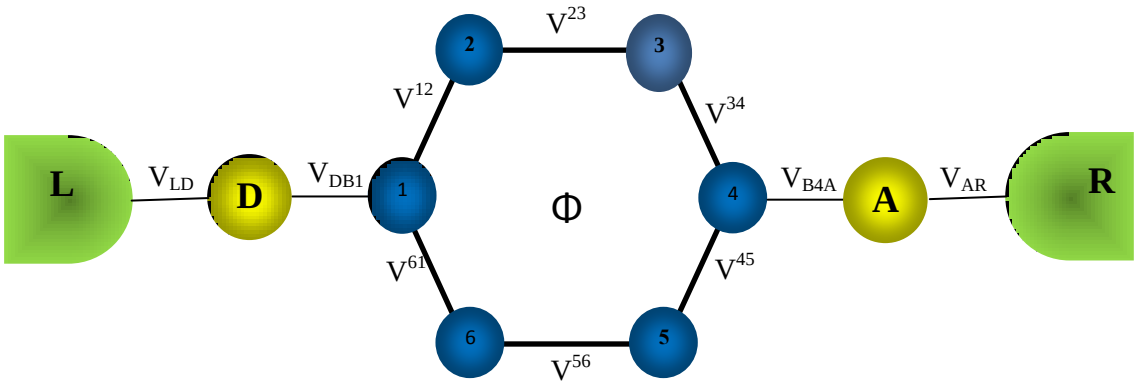

Fig. (1): The benzene ring model

This Hamiltonian is given by

$$\widehat{H}(t) = E_D n_D(t) + E_A n_A(t) + \sum_n E_{Bn} n_{Bn} + \sum_{k_L} E_{k_L} n_{k_L}(t) + \sum_{k_R} E_{k_R} n_{k_R}(t) + \left(V_{DB_1} C_D^\dagger(t) C_{B_1}(t) + H.C.\right) + \left(V_{AB_\ell} C_A^\dagger(t) C_{B_\ell}(t) + H.C.\right) + \sum_{n=1, m\neq n} \left(V_{B_n B_m} C_{B_n}^\dagger(t) C_{B_m}(t) + H.C.\right) + \left(V_{B_1 B_6} C_{B_1}^\dagger(t) C_{B_6}(t) + H.C.\right) + \sum_{k_L} \left(V_{Dk_L} C_D^\dagger(t) C_{k_L}(t) + H.C.\right) + \sum_{k_R} \left(V_{Ak_R} C_A^\dagger(t) C_{k_R}(t) + H.C.\right) \quad (1)$$

Where, $n_j(t) = C_j^\dagger(t) C_j(t)$ and the $C_j^\dagger(t)(C_j(t))$ denotes annihilation (creation) operators. The index k_i being a set of quantum numbers, with $i = L, R$. Notably, the summation in the third term in eq. (1) is over all quantum dots. While the sixth, seventh and eighth terms are concerning the coupling interactions between the donor/acceptor with all the quantum dots as well as between the quantum dots, respectively. In this formula, we consider the number 1 is the one that connected to the donor while the quantum dot number ℓ is the one that connected to acceptor.

For this model, three configurations are studied, the first is para configuration as the acceptor is connected to fourth dot, the second is meta configuration as the acceptor is connected to fifth dot, and the third is ortho configuration as the acceptor is connected to sixth dot. Therefore, the seventh term in eq.(1) is written in three forms depending on the configuration type,

$V_{AB4} C_A^\dagger(t) C_{B4}(t)$ for para configuration
$V_{AB5} C_A^\dagger(t) C_{B5}(t)$ for meta configuration
$V_{AB6} C_A^\dagger(t) C_{B6}(t)$ for ortho configuration

The equations of motion for $C_j(t)$ can be obtained by using [16],

$$\dot{C}_j(t) = -i \frac{d\widehat{H}(t)}{dC_j^\dagger(t)} \quad (2)$$

to get,

$$\dot{C}_D(t) = -iE_D C_D(t) - i \sum_{B_n} V_{DB_n} C_{B_n}(t) - i \sum_{k_L} V_{Dk_L} C_{k_L}(t) \quad (3)$$

$$\dot{C}_A(t) = -iE_A C_A(t) - i \sum_{B_n} V_{AB_n} C_{B_n}(t) - i \sum_{k_R} V_{Ak_R} C_{k_R}(t) \quad (4)$$

$$\dot{C}_{B_n}(t) = -iE_{B_n} C_{B_n}(t) - iV_{B_n D} C_D(t) - iV_{B_n A} C_A(t) - i \sum_{n=1, m\neq n} V_{B_n B_m} C_{B_m}(t) \quad (5)$$

$$\dot{C}_{k_L}(t) = -iE_{k_L} C_{k_L}(t) - iV_{k_L D} C_D(t) \quad (6)$$

$$\dot{C}_{k_R}(t) = -iE_{k_R} C_{k_R}(t) - iV_{k_R A} C_A(t) \quad (7)$$

For steady state we define $C_j(t)$ by the following:

$$C_j(t) = \bar{C}_j(E) e^{-iEt} \quad (8)$$

where E denotes the system eigenvalues, then accordingly, $\dot{\bar{C}}_J(E) = 0$.

In order to get logic and simple formula for the transmission probability amplitude, we assume the following energy separation procedure [8]:

$V_{k_B \alpha} = v_{k_B} V^{B\alpha}$; $V_{k_L D} = v_{k_L} V^{LD}$; $V_{k_R A} = v_{k_R} V^{RA}$; $\bar{C}_{k_\beta}(E) = v_{k_\beta} \bar{\bar{C}}_\beta$ (9)

Where $\alpha = D, A$ and $\beta = L, R, B$,then we get,

$$\frac{\bar{C}_A}{\bar{C}_D} = \frac{V^{AB_\ell}\Delta_{\ell D}/\Delta}{(E - E_A - V^{AB_\ell}\Delta_{\ell A}/\Delta) - \sum_{AR}(E)} \qquad for\ \ell = 4,5,6 \tag{10}$$

Where $\sum_{AR}(E)$ is the level self-energy [11],

$$\sum_{AR}(E) = |V^{AR}|^2\Gamma_R(E) = -i\Delta_{AR}(E) + \Lambda_{AR}(E) \tag{11}$$

Δ_{AR} (E) is the acceptor level broadening due to acceptor level-right lead's levels coupling interaction. Λ_{AR}(E) is the quantum shift that happens in the acceptor level due to the over mentioned coupling interactions. With [12],

$$\Delta_{AR}(E) = \pi|V^{AR}|^2\rho_R(E) \tag{12}$$

And,

$$\Lambda_{AR}(E) = P\frac{1}{\pi}\int \frac{\Delta_{AR}(E')}{E - E'}dE' \tag{13}$$

Where P refers to the principal part

For semi-infinite atomic chain for the leads, the density of electronic states for right lead is given by [21],

$$\rho_R(E) = \frac{1}{\pi|\beta_R|}\sqrt{1 - \left(\frac{E - E_{FR}}{2\beta_R}\right)^2} \tag{14}$$

Where E_{FR} is the position of Fermi energy level at the right lead. β_R is related to the occupied band width of the right lead.

The coupling interactions between the nearest neighbors dots in the presence of the magnetic flux are written as [22],

$V^{12}e^{i\phi/6}$,$V^{23}e^{i\phi/6}$,$V^{34}e^{i\phi/6}$, $V^{45}e^{i\phi/6}$, $V^{56}e^{i\phi/6}$ and $V^{61}e^{i\phi/6}$

Where the matrix equation is given by:

$$\begin{vmatrix} E-E_1 & -V^{12}e^{i\phi/6} & 0 & 0 & 0 & -V^{12}e^{i\phi/6} \\ -V^{21}e^{-i\phi/6} & E-E_2 & -V^{23}e^{i\phi/6} & 0 & 0 & 0 \\ 0 & -V^{32}e^{-i\phi/6} & E-E_3 & -V^{34}e^{i\phi/6} & 0 & 0 \\ 0 & 0 & -V^{43}e^{-i\phi/6} & E-E_4 & -V^{45}e^{i\phi/6} & 0 \\ 0 & 0 & 0 & -V^{54}e^{-i\phi/6} & E-E_5 & -V^{56}e^{i\phi/6} \\ -V^{12}e^{-i\phi/6} & 0 & 0 & 0 & -V^{65}e^{-i\phi/6} & E-E_6 \end{vmatrix} \times \begin{vmatrix} C_{B1} \\ C_{B2} \\ C_{B3} \\ C_{B4} \\ C_{B5} \\ C_{B6} \end{vmatrix} = \begin{vmatrix} V^{B1D}\bar{C}_D \\ 0 \\ 0 \\ V^{B4A}\bar{C}_A \\ V^{B5A}\bar{C}_A \\ V^{B6A}\bar{C}_A \end{vmatrix} \tag{15}$$

Where,

$$\Delta = \begin{vmatrix} E-E_1 & -V^{12}e^{i\phi/6} & 0 & 0 & 0 & -V^{12}e^{i\phi/6} \\ -V^{21}e^{-i\phi/6} & E-E_2 & -V^{23}e^{i\phi/6} & 0 & 0 & 0 \\ 0 & -V^{32}e^{-i\phi/6} & E-E_3 & -V^{34}e^{i\phi/6} & 0 & 0 \\ 0 & 0 & -V^{43}e^{-i\phi/6} & E-E_4 & -V^{45}e^{i\phi/6} & 0 \\ 0 & 0 & 0 & -V^{54}e^{-i\phi/6} & E-E_5 & -V^{56}e^{i\phi/6} \\ -V^{12}e^{-i\phi/6} & 0 & 0 & 0 & -V^{65}e^{-i\phi/6} & E-E_6 \end{vmatrix} \tag{16}$$

We can get Δ_{4A} (Δ_{4D}) by substituting the right side of eq. (15) in the fourth column of eq. (16), making $V^{B1D}\bar{C}_D = V^{B5A}\bar{C}_A = V^{B6A}\bar{C}_A = 0$ ($V^{B4A}\bar{C}_A = V^{B5A}\bar{C}_A = V^{B6A}\bar{C}_A = 0$), while we can get Δ_{5A} (Δ_{5D}) by substituting the right side of eq. (15) in the fifth column of eq. (16), making $V^{B1D}\bar{C}_D = V^{B4A}\bar{C}_A = V^{B6A}\bar{C}_A = 0$ ($V^{B4A}\bar{C}_A = V^{B5A}\bar{C}_A = V^{B6A}\bar{C}_A = 0$), and Δ_{6A} (Δ_{6D}) is solved by

substituting the right side of eq. (15) in the sixth column of eq. (16), making $V^{B1D}\bar{C}_D = V^{B4A}\bar{C}_A = V^{B5A}\bar{C}_A = 0$ ($V^{B4A}\bar{C}_A = V^{B5A}\bar{C}_A = V^{B6A}\bar{C}_A = 0$).

Then the transmission probability amplitude and transmission probability [9] can be calculated respectively as:

$$t(E) = \frac{\bar{C}_A(E)}{\bar{C}_D(E)} \quad (17)$$

$$T(E) = |t(E)|^2 \quad (18)$$

3- Calculations and Discussion

For all our results that presented in Figs.(2-4), the energy levels of the sites are chosen as $E_{B1}= E_{B2}=E_{B3}= E_{B4}= E_{B5}= E_{B6}=0$ and the coupling interaction between neighbors sites is V^{BB}=-0.5eV, $V^{DB} =V^{AB}$=-0.3eV, V^{AR}=-3.0eV, and β_R=-3.0eV . According to our results, we conclude the following:

1- In Fig. (2), the transmission spectrum for the three configurations is calculated in the absence of the magnetic flux. The transmission probability spectrum for each configuration has only four resonances, since $E = \mp 0.5eV$ are degenerate to pair of resonances. For meta configuration there is a single anti resonance at E=0, while there are two antiresonances for ortho configuration at $E = \mp 0.7eV$. The general conclusion is that the low transmission through the meta and ortho configurations result from destructive interference near the Fermi energy and $E = \mp 0.7eV$, respectively. Whereas the para configuration exhibits relatively large transmission through this region.

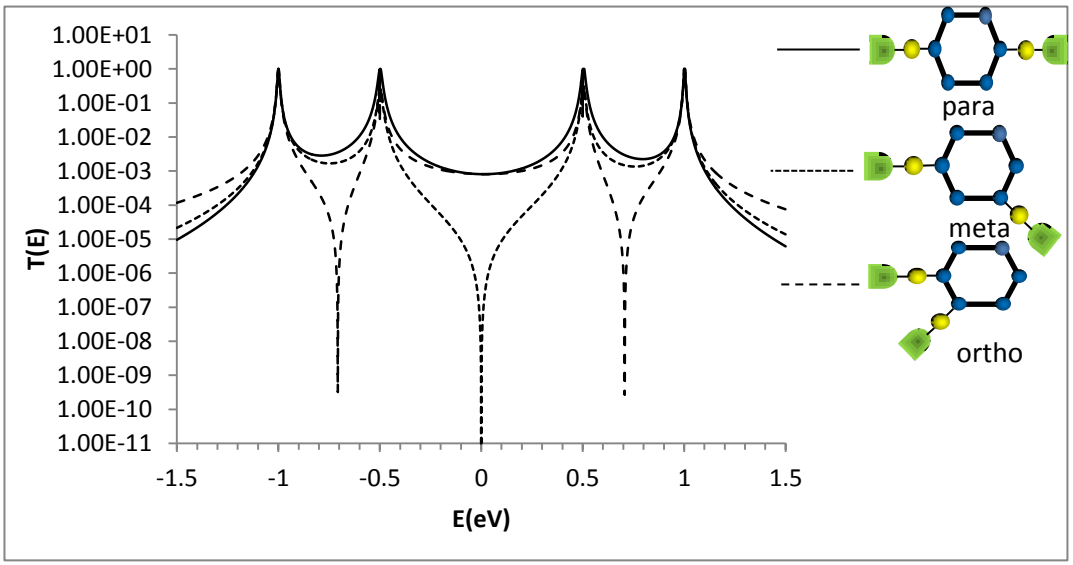

Fig.(2): the transmission probability as function of the system energy with $E_{B1}= E_{B2}=E_{B3}= E_{B4}= E_{B5}= E_{B6}=0$, $V^{DB}=V^{AB}$=-0.3eV, V^{BB}=-0.5eV, V^{AR}=-3eV, β_R=-3eV, ϕ=0.

2- In Figs. (3), the transmission spectrum for the three configurations are calculated in the presence of magnetic flux with $\phi = 0.3\pi, 0.6\pi \; and \; 0.9\pi$. It is obvious that the degeneracy is lifted by the magnetic field for all configurations. Two antiresonances appear at $E = \mp 0.5 \; eV$ for the para configuration. One anti resonance appears at E=0 for the meta configuration, while it disappears for the ortho one.

3- In Figs. (4), the transmission spectrum for the three configurations are calculated in the presence of magnetic flux with $\phi = n\pi(n\ is\ integer)$. For even n, four resonances appear at $E = \mp 0.5eV\ and\ \mp 1eV$ for all configurations. But the transmission probability is reduced at $E = \mp 0.5\ eV$ for the meta and ortho configurations. For odd n, the transmission spectrum is geometry dependent. The transmission probability is vanished in the case of para configuration. The number of resonances is reduced to three for the meta configuration, while it is reduced to two for the ortho configuration.

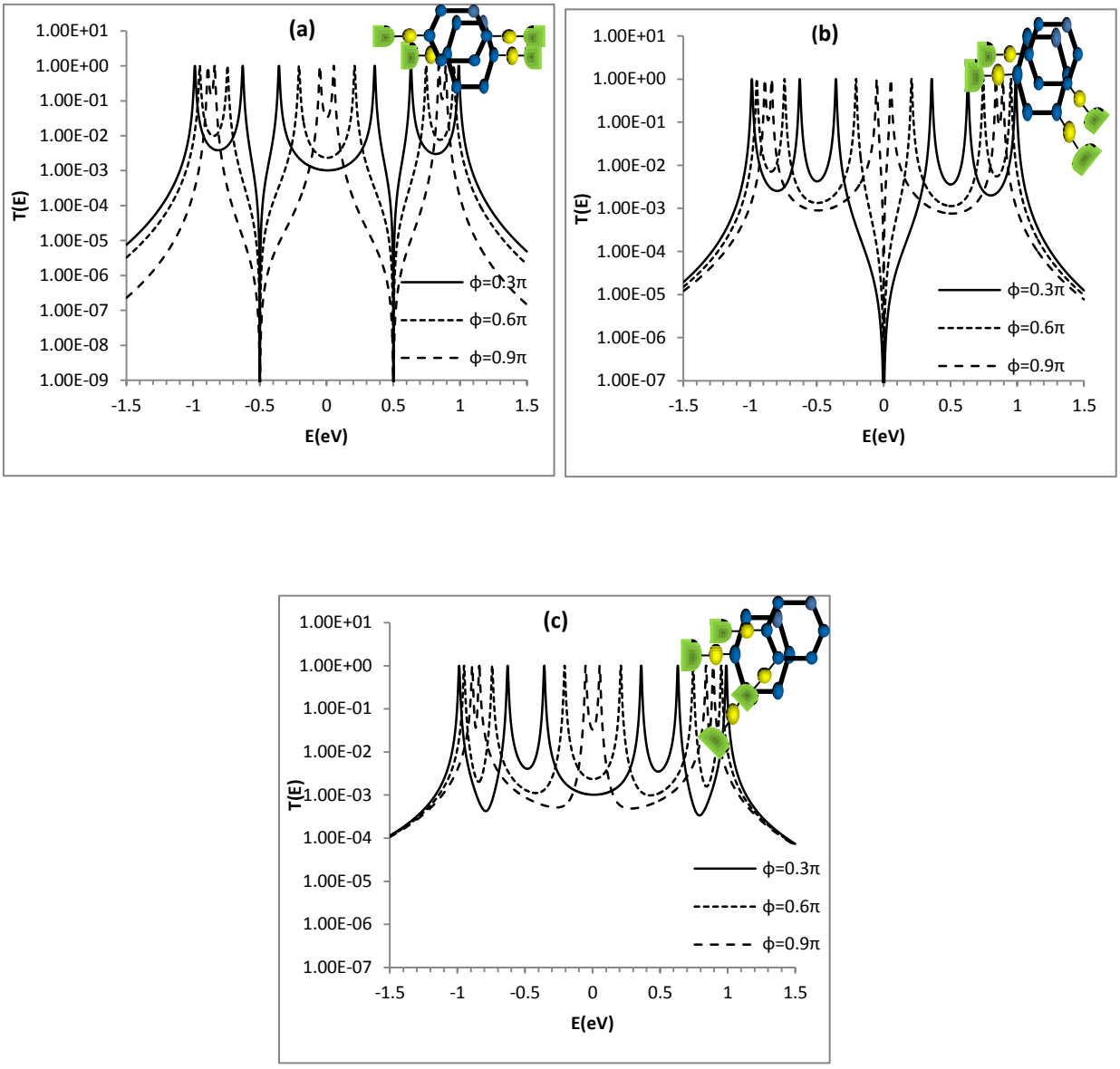

Fig.(3): The transmission probability as function of the system energy with presence magnetic flux at $\phi = 0.3\pi, 0.6\pi, 0.9\pi$ for three configurations are para in (a), meta in (b) and ortho in (c). The parameters are $E_{B1}= E_{B2}=E_{B3}= E_{B4}= E_{B5}= E_{B6}=0$, $V^{DB}=V^{AB}=-0.3eV$, $V^{BB}=-0.5eV$, $V^{AR}=-3eV$, $\beta_R=-3eV$.

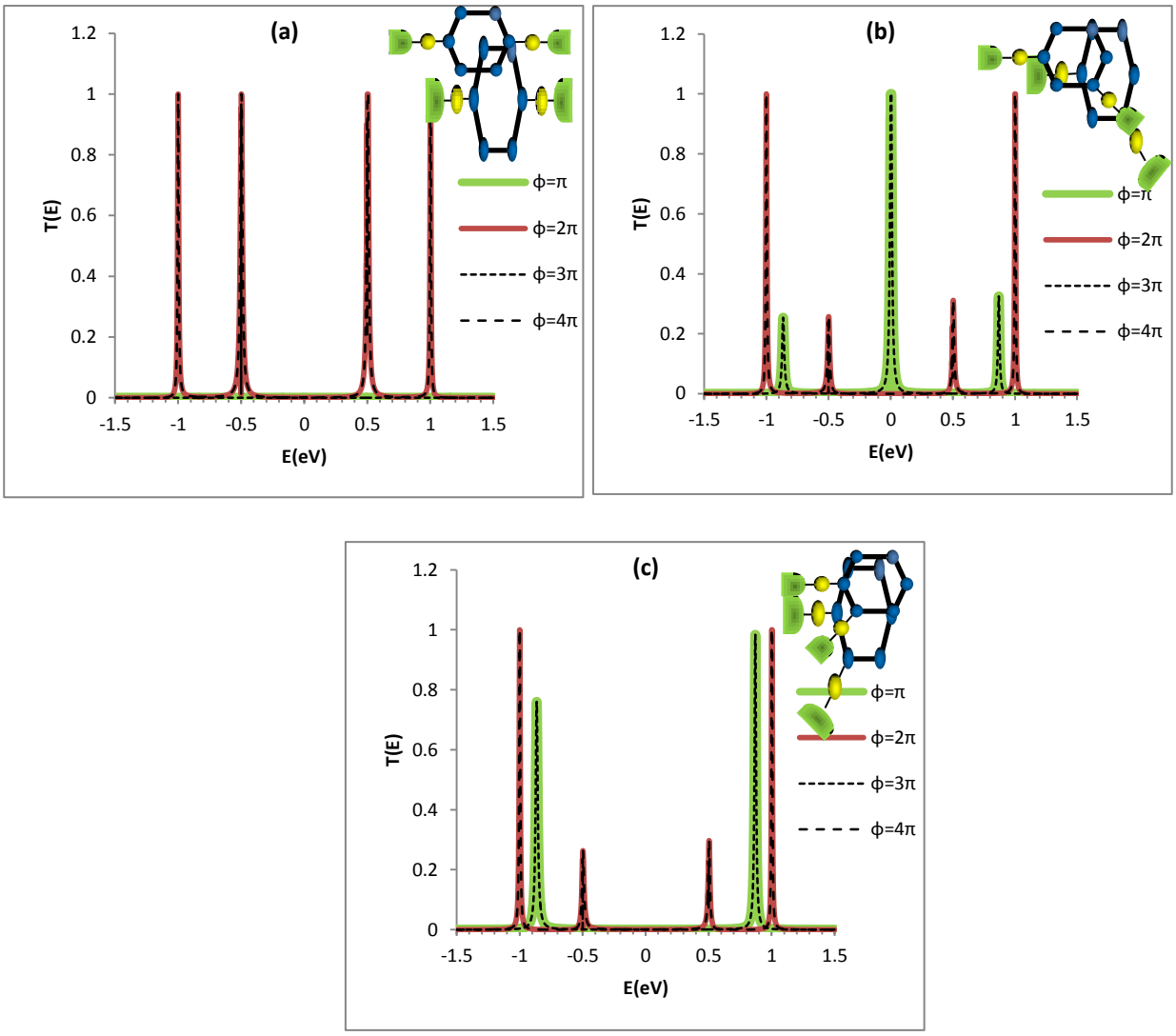

Fig.(4): The transmission probability as function of the system energy with presence magnetic flux at $\phi = \pi, 2\pi, 3\pi, 4\pi$ for three configurations are para in (a), meta in (b) and ortho in (c). The parameters are $E_{B1}= E_{B2}=E_{B3}= E_{B4}= E_{B5}= E_{B6}=0$, $V^{DB}=V^{AB}=-0.3eV$, $V^{BB}=-0.5eV$, $V^{AR}=-3eV$, $\beta_R=-3eV$.

Finally, according to our calculations, we conclude that the transmission spectrum is determined by two important (parameters). These are the magnetic field and the geometry of the scattering region which is determined by the contact's position of the acceptor of the ring. The transport properties for this system, considering the case of multi leads connections, will be investigated as a future work.

References

1- S. K. Maiti, Solid State Commun. **150**, 1269-1274, 2010.
2- Y. Okuno, and T. Ozaki, J. Phys. Chem. C **117**, 100−109, 2013.
3- M.-J. Li, H. Xu, K.-Q. Chen, M.-Q. Long, Phys. Lett. A **376**, 1692–1697, 2012.
4- S.-H. Ke, W. Yang and H. U. Baranger, Nano Lett. **8**, 3257, 2008.
5- S. R. J. Brueck and S. T. Picraux, " Implications of Emerging Micro- and Nanotechnologies", (National Academy of Sciences2003).
6- Tony Y. Abi-Salloum, Ph. D. Thesis, Drexel University, 2006.
7- A. Nishino, T. Imamura, and N. Hatano, J. Phys.: Conference Series **343**, 012087, 2012.
8- M. Büttiker1, and P. Samuelsson, Ann. Phys. (Leipzig) **16**, 751 – 766, 2007.
9- D. A. Lovey, S. S. Gomez, and R. H. Romero, http://arxiv.org/abs/ 1106.0407, 2011.
10- J.-M. Ma, J. Zhao, K.-C. Zhang, Y.-J. Peng and F. Chi, Nanoscale Reserch Letters **6**:265, 2011.
11- J.Zheng, F. Chi, X.-D. Lu and K.-C. Zhang, Nanoscale Research Letters, **7**,157, 2012.
12- Y.S. Liu, X.K. Hong, J.F. Feng and X.F. Yang, Nanoscale Research Letters, **6**:618, 2011.
13- G. Hackenbroich and H. A. Weidenmüller, Phys. Rev. Lett. **76**, 110, 1996.
14- J. Martin, T. Tritt, and C. Uher, J. Appl. Phys. **108**, 121101, 2010.
15- D. M. Newns, Phys. Rev. **178**, 3, 1969.
16- L. E. Ballentine, "Quantum Mechanic: A modern development", (World Scientific, Singapore), 2000.
17- C. Stampfi, N. Neugebauer and M. Schefiler, Surf. Sci. **8**, L307-L309, 501-506, 1994.
18- T. Ihn, 2010, "Semiconductor Nanostructures: Quantum States and Electronic Transport", Oxford University Press, New York.
19- M. Galperin, M. A. Ratner and A. Nitzan, J. Chem. Phys. **21**, 23, 2004.
20- D. M. Newns, K. Makoshi, R. Brako and J. N. M. Van Wannik, Physica Scripta,Vol. **T6**, 5-14, 1983.
21- K. W. Sulston, A. T. Amos and S. G. Davison, Surface Science, **179**, 555-566, 1988.
22- G. C. Solomon, D. Q. Andrews, T. Hansen, R. H. Goldsmith, M. R. Wasielewski, R. P. V. Duyne, and M. A. Ratner, J. Chem. Phys. **129**, 054701, 2008.